Autonomous dynamics of two-dimensional insulating domain with superclimbing edges

Anatoly Kuklov[®], Nikolay Prokof'ev[®], and Boris Svistunov[®]

¹Department of Physics and Astronomy, College of Staten Island and the Graduate Center of CUNY, Staten Island, New York 10314, USA

²Department of Physics, University of Massachusetts, Amherst, Massachusetts 01003, USA



(Received 30 April 2024; accepted 11 June 2024; published 1 July 2024)

Superclimbing dynamics is the signature feature of transverse quantum fluids describing wide superfluid one-dimensional interfaces and/or edges with negligible Peierls barrier. Using Lagrangian formalism, we show how the essence of the superclimb phenomeno—dynamic conjugation of the fields of the superfluid phase and geometric shape—clearly manifests itself via characteristic modes of autonomous motion of the insulating domain ("droplet") with superclimbing edges. In the translation invariant case and in the absence of supercurrent along the edge, the droplet demonstrates ballistic motion with the velocity-dependent shape and zero bulk currents. In an isotropic trapping potential, the droplet features a doubly degenerate sloshing mode. The period of the ground-state evolution of the superfluid phase (dictating the frequency of the AC Josephson effect) is sensitive to the geometry of the droplet. The supercurrent along the edge dramatically changes the droplet dynamics: The motion acquires features resembling that of a two-dimensional charged particle interacting with a perpendicular magnetic field. In a linear external potential (uniform force field), the state with a supercurrent demonstrates a spectacular gyroscopic effect—uniform motion in the perpendicular to the force direction.

DOI: 10.1103/PhysRevResearch.6.033008

I. INTRODUCTION

Recent progress in developing the theory of transverse quantum fluids (TQF)—quasi-one-dimensional edge superfluids featuring (at low enough temperature) stable persistent currents and off-diagonal long-range order thanks to their infinite effective compressibility enabled by the coupling to a particle reservoir in the transverse to the superflow direction [1–5]—was originally motivated by supertransport through a structurally imperfect crystal of ⁴He phenomena [6–14]. Lately, quantum fluctuations of the edge shape were systematically addressed and demonstrated to be as interesting and informative as superfluid properties [5]. For a review of all these activities, see Ref. [3].

The long-wave shape dynamics of the (microscopically) quantum rough superfluid edge stems from the superclimb effect—the edge motion in the direction transverse to its orientation supported by the supertransport of matter to/from the corresponding edge element [15]. (The word "climb" is used here in the full analogy to the text book terminology (see, e.g., Ref. [16]) indicating the nonconservative motion of dislocations). Quantitatively, the superclimbing dynamics is described by Hamiltonian formalism in which the field of the transverse (say, vertical) displacements of the edge is canonically conjugate to the field of the superfluid phase [15]. In other words, the role of the density as a conjugate variable to the phase (as explained in textbooks on superfluidity; see, e.g.,

Published by the American Physical Society under the terms of the Creative Commons Attribution 4.0 International license. Further distribution of this work must maintain attribution to the author(s) and the published article's title, journal citation, and DOI.

Ref. [17]) is played by the vertical displacement of the edge. At the quantum level, the ground-state and low-temperature fluctuations of the two fields are statistically coupled. This allows one to access superfluid properties of the edge by studying fluctuations of its shape [5]. In this work, we observe that there exists yet another—purely classical field—way of revealing the key aspects of the superclimbing dynamics, including the ones involving persistent-current states, through dynamics of the insulating domain with superclimbing edges. Such a domain in the system of hard-core bosons with the nearest-neighbor hopping and interaction terms on the square lattice is shown in Fig. 1 (numerous alternative setups are mentioned in Sec. VI). To be more specific, the self-bound domain state is described by the Hamiltonian

$$H_{\rm hc} = -t \sum_{\langle i,j \rangle} b_j^{\dagger} b_i + V \sum_{\langle i,j \rangle} n_j n_i - \mu \sum_i n_i, \tag{1}$$

where V<-2t, b_i is the bosonic annihilation operator and occupation numbers obey $n_i\leqslant 1$, and μ stands for the chemical potential. It can be rewritten identically as the easy-axis spin-1/2 ferromagnetic model with $J_x=J_y=2t$ and $J_z=-V$, and μ playing the role of the magnetic field. The width of the domain edge and its superfluid stiffness are controlled by the nearest-neighbor attraction and diverge at $V\to -2t$. As demonstrated in Ref. [5], when the edge width exceeds several lattice periods, the edge enters the TQF regime when the Peierls barrier can be neglected on exponentially large scales—much larger than the domain perimeter. Under these conditions, the discrete translation symmetry and the square lattice discrete rotation symmetry become irrelevant as well and the equilibrium domain shape is expected to be a perfect circle (see Fig. 1).

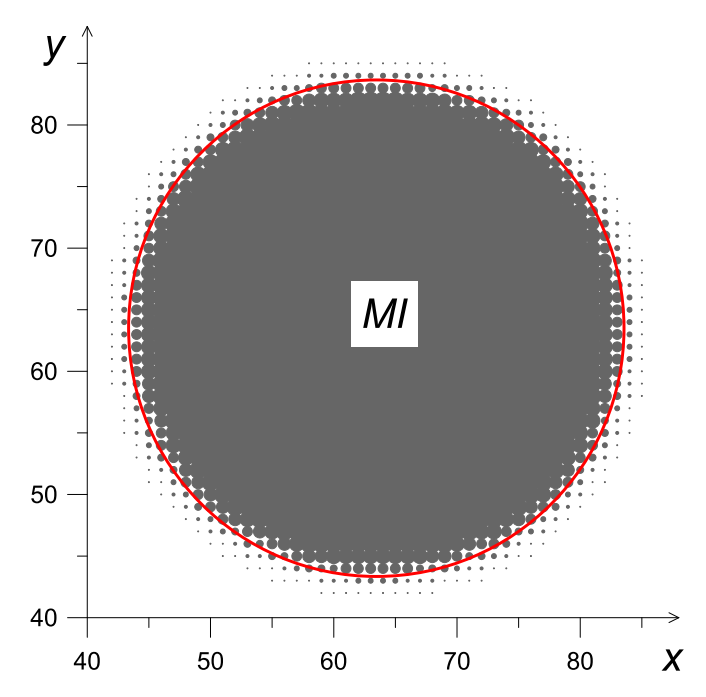


FIG. 1. Insulating domain with 1260 particles in model (1) at V = -2.2t (symbol sizes are proportional to the average occupation number). Simulations were performed at temperature T = t/128. The red line is a circle used for better visualization of the domain shape. By symmetry, a void in the insulator occupying the outer space has the same properties.

The emergent (upon coarse-graining) translational invariance guarantees that the droplet can perform ballistic motion with velocity-dependent shape in the absence of bulk currents. The droplet confined by an isotropic external potential has to demonstrate a doubly degenerate sloshing mode. In the presence of persistent current around the droplet edge, the degeneracy of the sloshing mode is lifted, and the sloshing motion is accompanied by Foucault-like precession. In a linear external potential (uniform force field), the state with a supercurrent demonstrates a spectacular gyroscopic effect—uniform motion in the perpendicular to the force direction.

II. THE MODEL

Quantitative analysis is conveniently performed with the Lagrangian formalism in terms of the edge position, $\mathbf{r}(\xi,t) = (x(\xi,t),y(\xi,t))$, and the superfluid phase along the edge, $\phi(\xi,t)$, as functions of time t, with parameter ξ labeling the edge points. The structure of the Lagrangian readily follows from the continuity equation, the form of the latter expressing the law of conservation of matter under specific conditions of (i) supertransport along the edge and (ii) insulating incompressible bulk.

A. Parametrization freedom

Formally, it is convenient to view the three functions $x(\xi,t), y(\xi,t), \phi(\xi,t)$ as dynamical fields despite that there should be only two conjugate variables. The redundancy in this approach is associated with the parametrization freedom. If $\mathbf{r}(\xi,t), \phi(\xi,t)$ is a solution to our dynamic problem, then,

treating parameter ξ as an *arbitrary* function of a new parameter, ξ' , and time, that is, substituting $\xi \equiv \xi(\xi',t)$ into the solution, we get an equivalent solution, $\mathbf{r}'(\xi',t)$, $\phi'(\xi',t)$, where

$$\mathbf{r}'(\xi',t) = \mathbf{r}(\xi(\xi',t),t), \quad \phi'(\xi',t) = \phi(\xi(\xi',t),t).$$
 (2)

Thus, for the three variables, there should be only two physical equations of motion, with a freedom of choosing this or that condition fixing the "gauge," which is by selecting a specific parametrization.

In most cases, one would *ultimately* prefer to work with two rather than three unknown functions using parametrization of the following type:

$$x(\xi, t) = X(\eta(\xi, t), \xi, t), \quad y(\xi, t) = Y(\eta(\xi, t), \xi, t).$$
 (3)

Here, $X(\eta, \xi, t)$ and $Y(\eta, \xi, t)$ are certain fixed functions of three variables and $\eta(\xi, t)$ is the unknown field conjugate (but not necessarily canonically) to the field $\phi(\xi, t)$. A very important practical example of parametrization (3) is the polar coordinate system with a moving origin:

$$x(\theta, t) = x_0(t) + r(\theta, t)\cos\theta,\tag{4}$$

$$y(\theta, t) = y_0(t) + r(\theta, t)\sin\theta, \tag{5}$$

where the radius $r(\theta, t)$ plays the role of the function $\eta(\xi, t)$ with $\xi \equiv \theta$.

Fixing the gauge by Eq. (3) can be implemented at three different stages. Option 1 is to introduce the Lagrangian or Hamiltonian description directly in terms of two rather than three fields. Such an approach was used in Ref. [15], where the role of parameter ξ was played by the coordinate x, in which case the field y(x) was argued to be canonically conjugate to the field $\phi(x)$. Along similar lines, in polar coordinates, identifying parameter ξ with the polar angle θ , one can see that the variable canonically conjugate to $\phi(\theta)$ is one half of the square of the polar radius, $r^2(\theta)/2$. This observation then immediately leads to the Hamiltonian of the system.

More flexible is Option 2, where one formulates a generic Lagrangian in terms of the three fields, $x(\xi)$, $y(\xi)$, $\phi(\xi)$, and then substitutes Eq. (3) into the Lagrangian to get a gauge-specific Lagrangian in terms of $\phi(\xi)$ and $\eta(\xi)$. Even more flexible is Option 3, where the substitution (3) is implemented at the level of the generic equations of motion, obtained from the generic Lagrangian, or otherwise not used at all, so that the gauge is fixed by a different protocol explained in Sec. II B.

B. Covariant representation

Gauge redundancy associated with the parametrization freedom implies that the system of three equations of motion following from the generic Lagrangian should be degenerate: One should be able to reduce it to two independent—and incomplete in view of the gauge freedom—equations and a trivial identity. From superfluid hydrodynamics, it is clear that the system of two independent equations can be cast into the form when one of them is the continuity equation expressing the law of conservation of matter and the other one is the generalized Beliaev–Josephson–Anderson (BJA) equation describing the time evolution of the field ϕ . In what follows, we

will see that this is indeed the case. Meanwhile, it is important to discuss the optimal representation of these equations.

We want the two dynamic equations to be maximally insensitive (covariant) with respect to the choice of parametrization. To this end, we employ the tools of differential geometry. Let l be the (algebraically understood) arc length, with its infinitesimal element being

$$dl = l_{\xi} d\xi, \quad l_{\xi} = \sqrt{x_{\xi}^2 + y_{\xi}^2}$$
 (6)

 $(x_{\xi} \equiv \partial_{\xi} x, y_{\xi} \equiv \partial_{\xi} y, \partial_{\xi} \equiv \partial/\partial \xi)$. The unit vectors

$$\hat{\mathbf{n}} = l_{\xi}^{-1}(y_{\xi}, -x_{\xi}), \quad \hat{\mathbf{t}} = l_{\xi}^{-1}(x_{\xi}, y_{\xi}),$$
 (7)

are normal and tangent to the line, respectively. We will also need the signed line curvature $(x_{\xi\xi} \equiv \partial_{\xi}^2 x, y_{\xi\xi} \equiv \partial_{\xi}^2 y)$:

$$\kappa = l_{\xi}^{-3} (x_{\xi} y_{\xi\xi} - y_{\xi} x_{\xi\xi}). \tag{8}$$

Finally, an important role will be played by the arc length derivative:

$$\partial_l = l_{\varepsilon}^{-1} \partial_{\xi}. \tag{9}$$

The vectors $\hat{\bf n}$ and $\hat{\bf t}$, the scalar κ , and the operator ∂_l have purely geometric meaning rendering them covariant. Expressing the two dynamic equations in terms of these objects leaves potentially noncovariant only the terms with time derivatives: $\dot{\bf r}$ and $\dot{\phi}$.

Considering time derivatives, our first observation is that the scalar $\hat{\bf n}\cdot\dot{\bf r}$ is also gauge invariant. This can be shown purely mathematically but is also immediately clear from the physical meaning of this quantity—the velocity of the displacement of the edge in the vertical direction. Our second observation is that the scalar $\hat{\bf t}\cdot\dot{\bf r}$ definitely depends of the gauge and by no means can be unambiguously defined unless some extra (gauge-fixing) condition is applied. Indeed, the meaning of this quantity is the velocity of the motion of the label ξ along the edge. There are absolutely no physical consequences associated with this "motion" leaving the shape of the edge intact. But there is a mathematical consequence—a "conspiracy" between $\hat{\bf t}\cdot\dot{\bf r}$, $\dot{\phi}$, and $\partial_l\phi$ that can be cast in the form of the invariance with respect to the gauge transformation,

$$\hat{\mathbf{t}} \cdot \dot{\mathbf{r}} \to \hat{\mathbf{t}} \cdot \dot{\mathbf{r}} + g(\xi, t),$$
 (10)

$$\dot{\phi} \rightarrow \dot{\phi} + g(\xi, t) \, \partial_t \phi,$$
 (11)

where $g(\xi,t)$ is an arbitrary function; in terms of the reparametrization (2), it is expressed as $g=l_{\xi}\dot{\xi}(\xi',t)$. The meaning of the transformation (10)–(11) is purely geometrical (and, in particular, has nothing to do with the physical meaning of ϕ). The transformation expresses the rather obvious fact that the motion of the label along the line creates an apparent contribution to time derivatives of the fields proportional to the velocity $\hat{\bf t} \cdot \dot{\bf r}$ and the arc gradient of the field.

Hence, if all time derivatives in the (otherwise covariant) equations of motion are expressed in terms of $\hat{\bf n}\cdot\dot{\bf r}$, $\hat{\bf t}\cdot\dot{\bf r}$, and $\dot{\phi}$, then $\dot{\phi}$ and $\hat{\bf t}\cdot\dot{\bf r}$ have to enter the equations of motion in the form of

$$\dot{\phi} - (\hat{\mathbf{t}} \cdot \dot{\mathbf{r}}) \, \partial_l \phi$$
 (covariant time derivative). (12)

Furthermore, since the time derivative of $\dot{\phi}$ is not the part of continuity equation, the term (12) should enter only the BJA equation.

Gauge-invariance relations (10)–(11) suggest the following on-the-fly gauge-fixing protocol, which appears to be quite appropriate for numeric simulations. In this protocol, one assigns any desired value, including zero, to the longitudinal velocity $\hat{\mathbf{t}} \cdot \dot{\mathbf{r}}$ at the time t and parameter ξ . The covariant time derivative (12) in the BJA equation then automatically assigns the matching value to $\dot{\phi}$.

C. Continuity equation

The superfluid current along the edge is given by

$$j = n_s \partial_l \phi, \tag{13}$$

where n_s is the superfluid stiffness. As long as we are interested in the regime of an appropriately wide edge and not so large values of j, we can safely treat n_s as a constant. (Otherwise, we would need to take into account the dependence of n_s on j, as well as on the line orientation and curvature.)

The divergence of the superfluid current, $\partial_l j$, yields the local (and algebraically understood) accumulation of matter. Since the bulk is incompressible, the edge shifts accordingly in the transverse direction and the matter balance is expressed by the *continuity equation*:

$$\hat{\mathbf{n}} \cdot \dot{\mathbf{r}} + \partial_t j = 0 \quad \Leftrightarrow \quad \hat{\mathbf{n}} \cdot \dot{\mathbf{r}} = -n_s \partial_t^2 \phi. \tag{14}$$

Here and in what follows the unit of length is defined by the condition that the two-dimensional particle number density in the bulk equals unity.

Integrating Eq. (14) over the total arc length yields the law of conservation of the area of the droplet, A:

$$\mathcal{A} = \frac{1}{2} \oint dl \,\hat{\mathbf{n}} \cdot \mathbf{r},\tag{15}$$

$$\frac{d\mathcal{A}}{dt} = \oint dl \,\hat{\mathbf{n}} \cdot \dot{\mathbf{r}} \propto \oint dl \,\partial_l j \equiv 0. \tag{16}$$

D. Lagrangian

The total energy of the system,

$$E_{\text{tot}}[\phi, \mathbf{r}] = E_{\text{SF}}[\phi, \mathbf{r}] + E_{\text{cnf}}[\mathbf{r}], \tag{17}$$

splits into two distinct parts: the kinetic energy of superfluid currents,

$$E_{\rm SF}[\phi, \mathbf{r}] = \frac{n_s}{2} \oint dl (\partial_l \phi)^2, \tag{18}$$

and the configurational energy, which, in a general case of external potential, includes two terms:

$$E_{\rm cnf}[\mathbf{r}] = \chi \oint dl + E_{\rm pot}[\mathbf{r}]. \tag{19}$$

The first term is proportional to the total arc length. As it was done previously with n_s , we ignore the effects of curvature, anisotropy, etc., and treat χ as a constant. The second term is the potential energy of the droplet in an external potential, $U(\mathbf{r}')$:

$$E_{\text{pot}} = \int_{\Delta} U(\mathbf{r}') d^2 r' \tag{20}$$

(the integration is over the position \mathbf{r}' inside the droplet area).

To produce the Lagrangian, we need to combine the energy with the term conjugating superfluid phase field to the edge shape degrees of freedom. The structure of this term can be guessed based on the special case of an almost straight edge with the parametrization $\phi \equiv \phi(x)$, $y \equiv y(x)$ considered in Ref. [15]. In this case, the conjugating term has the form $\int dx \phi \dot{y}$ suggesting a straightforward generalization to

$$\oint dl \, \phi \, \hat{\mathbf{n}} \cdot \dot{\mathbf{r}} = \int \phi(y_{\xi} \dot{x} - x_{\xi} \dot{y}) \, d\xi, \tag{21}$$

thus leading to the Lagrangian

$$\mathcal{L} = \oint dl \, \phi \, \hat{\mathbf{n}} \cdot \dot{\mathbf{r}} - E_{\text{tot}}[\phi, \mathbf{r}]. \tag{22}$$

The validation of the correctness of the form of the first term of Lagrangian (22) comes from the fact that variation over ϕ correctly reproduces continuity equation (14).

E. Central potential

Of particular interest is the case of central potential $U(\mathbf{r}) = U(r)$, where polar parametrization (4)–(5) with $x_0(t) = y_0(t) = 0$ is the most natural. In this case, Lagrangian (22) takes the form

$$\mathcal{L} = -\oint d\theta \left[\frac{\dot{\phi}r^2}{2} + \frac{n_s\phi_\theta^2}{2\sqrt{r_\theta^2 + r^2}} + \chi\sqrt{r_\theta^2 + r^2} + \Lambda(r) \right],\tag{23}$$

$$\Lambda(r) = \int_0^r U(r')r'dr'. \tag{24}$$

Note that (as already mentioned) the variable $r^2/2$ is canonically conjugate to ϕ .

F. Generalized BJA equation

Observing that the variation of the term $E_{pot}[\mathbf{r}]$ with respect to the edge position can be written as

$$\delta E_{\text{pot}}[\mathbf{r}] = \oint (y_{\xi} \delta x - x_{\xi} \delta y) U(x(\xi), y(\xi)) d\xi, \qquad (25)$$

we then find that variations of (22) with respect to x and y yield, respectively, two equations:

$$-\dot{\phi}y_{\xi} + \dot{y}\phi_{\xi} - \partial_{\xi} \left[\left(\frac{n_{s}\phi_{\xi}^{2}}{2l_{\xi}^{3}} - \frac{\chi}{l_{\xi}} \right) x_{\xi} \right] - y_{\xi}U = 0, \quad (26)$$

$$\dot{\phi}x_{\xi} - \dot{x}\phi_{\xi} - \partial_{\xi} \left[\left(\frac{n_{s}\phi_{\xi}^{2}}{2l_{\xi}^{3}} - \frac{\chi}{l_{\xi}} \right) y_{\xi} \right] + x_{\xi}U = 0. \tag{27}$$

Multiplying (26) by x_{ξ} and (27) by y_{ξ} and then adding the results produces the anticipated identity, if the continuity equation (14) is taken into account. Multiplying (26) by y_{ξ} and (27) by x_{ξ} and then subtracting the results, we obtain the the BJA relation as

$$\dot{\phi} - (\hat{\mathbf{t}} \cdot \dot{\mathbf{r}}) \, \partial_l \phi = \kappa(\mathbf{r}) \left[\frac{n_s}{2} (\partial_l \phi)^2 - \chi \right] - U(\mathbf{r}). \tag{28}$$

Note the covariant form of this equation.

III. NON-GALILEAN BALLISTICS

Here we are interested in the motion of the droplet as a whole, that is, without changing its shape in time. In what follows, we will consider the case $\dot{r}=0$ in the parametrization (4)–(5) and use the reference frame of the stationary lattice unless otherwise specified. With the equations of motion (14) and (28), we can readily prove (by contradiction) the absence of Galilean ballistics of the droplet. As a by-product, we will establish that the droplet will perform a uniform motion while having a circular shape only in the presence of the fine-tuned external potential in the transverse to the motion direction.

Suppose we have a circular droplet of radius r = R = const moving along the *x*-axis with the velocity v_0 . In Eq. (5), we then have $y_0 = 0$, $x_0 = v_0 t$, that is, $\hat{\mathbf{n}} \cdot \dot{\mathbf{r}} = v_0 \cos \theta$ and $\partial_t = R^{-1} \partial \theta$, so that Eq. (14) implies

$$\phi(\theta, t) = \frac{v_0 R^2}{n_s} \cos \theta + M\theta - \mu t, \qquad (29)$$

where M is the phase winding number and μ is a certain constant. If the lattice frame of reference—the one we work in—is inertial, then M is an integer. If the lattice rotates with angular velocity Ω , then in its reference frame integer values of M have to be shifted by $\Delta M = \varphi_0/(2\pi) = m_0 \Omega R^2$, where m_0 is the particle mass and $\varphi_0 \in [-\pi, \pi]$ is the rotation-induced phase shift; here and in what follows, we set $\hbar = 1$. The dependence on φ_0 adds a gyrometric aspect to the problem. Linearity of the time-dependent additive term in (29) is required by consistency with the time-independent r.h.s. of Eq. (28).

Substitution of $\phi(\theta, t)$ of Eq. (29) into Eq. (28) shows that there should be a fine-tuned external potential

$$U(y) = \frac{3v_0^2 y^2}{2n_r R} - \frac{2Mv_0 y}{R^2},\tag{30}$$

and the constant has been dropped.

The M=0 result reveals inconsistency between the uniform motion and circular droplet shape in the absence of the external potential. To satisfy Eq. (28) at low velocity,

$$v_0 \ll \frac{\sqrt{n_s \chi}}{R},\tag{31}$$

one has to assume small deformation of the droplet shape (and thus its curvature), $r(\theta) = R - \epsilon f(\theta)$. Keeping only linear in ϵ terms in (28), we obtain

$$\epsilon = \frac{v_0^2 R^3}{4n_s \chi} \ll R, \quad f = \cos(2\theta),$$
 (32)

that is, in the absence of external potential, the distortion of the circular shape (elongation in the y-direction) of the moving droplet (with M=0) vanishes quadratically with v_0 at $v_0 \to 0$. The parabolic confining potential in (30) is required to "compress" the droplet back to its circular shape. From the flow kinetic energy, $E_{\rm SF} = \pi R^3 v_0^2/2n_s$, we also obtain the droplet effective mass as

$$m_{\text{eff}} = \frac{\pi R^3}{n_s} + \mathcal{O}(\epsilon^2). \tag{33}$$

The same result follows from the analysis of the sloshing mode considered in Sec. V. When the condition (31) is violated, the superflow at the edge is no longer protected by small parameters against either quantum phase slips or dynamic spectrum instability [2]; in addition, at such values of v_0 , the bilinear in $\partial_l \phi$ form of $E_{\rm SF}$ cannot be justified.

The $M \neq 0$ case is fundamentally different. To begin with, in the absence of external potential, it is impossible to satisfy Eq. (28) by deforming the droplet shape: Mathematically, the problem reduces to solving equation

$$f + f_{\theta\theta} = -3\cos(2\theta) + b\sin\theta$$

which has no 2π -periodic solutions when $b \propto M$ is nonzero. In other words, persistent current at the droplet edge eliminates the possibility of the ballistic propagation in free space! Uniform motion at the velocity v_0 along x becomes possible, if both the droplet deformation

$$r = R - \epsilon \cos(2\theta) \tag{34}$$

occurs and the uniform force

$$F = \frac{2Mv_0}{R^2},\tag{35}$$

with U = -Fy along y is applied. [It is assumed that $M^2n_s/(2\chi R^2) \ll 1$]. It is worth mentioning that such linear potential can be induced by accelerating the whole lattice.

Of special interest is the case U=0, $M \neq 0$. As shown previously, no uniform motion is possible in this case. The solution to the system of Eqs. (14) and (28) exits when the droplet performs a centripetal motion with some radius R_c at some angular velocity ω_c and simultaneously is deformed. We consider the case of small deformation $r = R - \epsilon f(\theta)$. Then we find $\hat{\mathbf{n}} \cdot \mathbf{r} = R_c \omega_c \sin(\theta - \omega_c t)$ and $\hat{\mathbf{t}} \cdot \mathbf{r} = R_c \omega_c \cos(\theta - \omega_c t)$. The continuity equation gives $\phi = (R_c \omega_c R^2/n_s) \sin(\omega - \omega_c t) + M\theta - \mu t$. Substituting ϕ into Eq. (28) gives

$$r = R - \frac{(R_c \omega_c)^2 R^3 \cos[2(\theta - \omega_c t)]}{4n_s \chi} + \mathcal{O}(\epsilon^2)$$
 (36)

and

$$\omega_c = \frac{2Mn_s}{R^3}. (37)$$

This situation resembles centripetal motion of a particle with mass (33) carrying some charge q in the magnetic field $B = 2\pi M/q$.

IV. GROUND-STATE SOLUTION AND AC JOSEPHSON EFFECT

As in any superfluid, the ground state of the droplet features broken time-translation symmetry—the time-crystallization effect—manifested by the linear growth of the phase with time:

$$\dot{\phi} = -\mu. \tag{38}$$

where $\mu = dE/dN$ is the chemical potential that depends on the area and shape of the droplet, with E from Eqs. (23)–(24) differentiated with respect to $N = \pi r^2$ for the case $r_\theta = 0$. The latter is sensitive to the presence of anisotropic trapping potential, in which case the shape also becomes sensitive

to the presence of the supercurrent. The continuity equation states that the phase gradient along the edge is constant:

$$\partial_l \phi = \zeta. \tag{39}$$

The two parameters, μ and ζ , control the shape of the droplet via the stationary BJA equation:

$$\left(\chi - \frac{n_s \zeta^2}{2}\right) \kappa(\mathbf{r}) + U(\mathbf{r}) = \mu. \tag{40}$$

In the general case of an anisotropic potential $U(\mathbf{r})$ and nonzero supercurrent, the parameter ζ can be viewed at the eigenvalue of the problem at a given value of μ . It has to satisfy the phase winding quantization condition

$$\zeta \oint dl = 2\pi M. \tag{41}$$

(Equivalently, μ can be viewed as an eigenvalue of the problem at a given value ζ .) For a given phase winding M, we thus get a single-parametric family of solutions controlled by the pair $(\mu, \zeta_M(\mu))$ that implicitly defines the shape of the droplet as a function of the total amount of matter and M.

In the case of isotropic potential, the situation is quite simple. The droplet has a circular form, meaning that $\kappa = 1/R$ and $\zeta = M/R$, where R is the radius of the droplet. Eq. (40) then simply relates μ to R and M:

$$\mu = U(r) + \frac{1}{R} \left(\chi - \frac{n_s M^2}{2R^2} \right). \tag{42}$$

V. NORMAL MODES: EFFECT OF A SUPERCURRENT

To find normal modes of a circular droplet of radius R trapped in a rotationally symmetric potential, we need to linearize equations of motion in the vicinity of the equilibrium solution with μ given by Eq. (42). This is done by substituting

$$\phi(\theta, t) = -\mu t + M\theta + \varphi(\theta, t), \tag{43}$$

$$r(\theta, t) = R + h(\theta, t), \tag{44}$$

either into equations of motion (14) and (28) or directly into the Lagrangian (23). In the latter case, implemented in the following, the linear in φ and h terms automatically nullify and the resulting bilinear Lagrangian generates the desired pair of linear in φ and h dynamic equations describing the normal modes, including the ballistic motion in the absence of the trapping potential.

The bilinear Lagrangian reads

$$\mathcal{L}_{bl} = -R \oint d\theta \left[\dot{\varphi}h + \frac{A\varphi_{\theta}^2}{2} - B\varphi_{\theta}h + \frac{Ch_{\theta}^2}{2} + \frac{Dh^2}{2} \right], \quad (45)$$

$$A = \frac{n_s}{R^2}, \quad B = \frac{n_s M}{R^3}, \tag{46}$$

$$C = \frac{\chi}{R^2} - \frac{n_s M^2}{2R^4}, \quad D = U'(R) - \frac{\chi}{R^2} + \frac{3n_s M^2}{2R^4}.$$
 (47)

The solution to the equations of motion,

$$\dot{h} + A\varphi_{\theta\theta} - Bh_{\theta} = 0, \tag{48}$$

$$\dot{\varphi} - B\varphi_{\theta} - Ch_{\theta\theta} + Dh = 0, \tag{49}$$

is a linear combination of normal modes

$$h_m = \operatorname{Re} \alpha_m e^{im\theta - i\omega_m^{\pm}t}, \quad \varphi_m = \operatorname{Re} \beta_m e^{im\theta - i\omega_m^{\pm}t}$$
 (50)

$$\omega_m^{\pm} = Bm \pm m\sqrt{A(m^2C + D)}, \quad m = 1, 2, 3, \dots$$
 (51)

With Eqs. (46)–(47), we have

$$\omega_m^{\pm} = \frac{mn_sM}{R^3} \pm m\sqrt{\frac{n_sU'(R)}{R^2} + \frac{n_s^2M^2}{R^6} + \frac{(m^2 - 1)n_s\tilde{\chi}}{R^4}}, (52)$$

where

$$\tilde{\chi} = \chi - \frac{n_s M^2}{2R^2} \tag{53}$$

is a renormalized (due to the supercurrent) parameter χ . In what follows, we assume that this renormalization is small because the condition

$$|M| \ll \sqrt{\chi/n_s} R \tag{54}$$

protects supercurrent states from quantum phase slips.

A. Fundamental modes

Of special interest are fundamental solutions corresponding to m = 1. Their frequencies do not depend on χ but do depend on M:

$$\omega_1^{\pm} = \frac{n_s M}{R^3} \pm \sqrt{\frac{n_s}{R^2} \left[U'(R) + \frac{n_s M^2}{R^4} \right]}.$$
 (55)

In the absence of supercurrents, both frequencies are equal (up to the global sign) and the fundamental solution corresponds to the doubly degenerate sloshing mode with frequency

$$\omega_{\rm sl} = \frac{\sqrt{n_s U'(R)}}{R}.$$
 (56)

In the limit of $U'(R) \to 0$, this mode corresponds to ballistic motion with near-circular droplet shape; in other words, it is identical to that of a point particle with effective mass (33) in the potential $\pi R^2 U(r)$.

Supercurrent qualitatively changes the picture of motion. The two frequencies become different leading to two characteristic regimes controlled by the value of the parameter

$$\gamma = \frac{|M|}{R^2} \sqrt{\frac{n_s}{U'(R)}}. (57)$$

At $\gamma \ll 1$, the relative difference between the magnitudes of the two frequencies is small:

$$|\omega_1^{\pm}| = \omega_{\rm sl}(\sqrt{1+\gamma^2} \pm \gamma). \tag{58}$$

Here we are dealing with the previously discussed sloshing mode that now demonstrates slow Foucault-type precession.

In the regime $\gamma \gg 1$, we have $|\omega_1^-| \ll |\omega_1^+|$:

$$|\omega_1^{\pm}| = \omega_* \frac{\sqrt{1 + \gamma^{-2}} \pm 1}{2}, \quad \omega_* = \frac{2n_s|M|}{R^3}.$$
 (59)

Here, the motion is similar to that of a two-dimensional charged particle in perpendicular to the plane magnetic field and weak harmonic trap. In particular, this means that there is no ballistic motion at $M \neq 0$. Indeed, in the absence of the external potential, $|\omega_1^+| = \omega_*$ and $\omega_1^- = 0$, implying that

the center of mass performs uniform circular motion with the angular frequency ω_* .

B. Modes with $m \gg 1$

At $m \gg 1$, we can neglect the middle term under the square root in Eq. (52) because inequality (54) guarantees that it is small and is getting progressively less relevant with increasing m, and omit 1 compared to m^2 :

$$|\omega_m^{\pm}| \to m \sqrt{\frac{n_s}{R^2} \left[U'(R) + \frac{m^2 \tilde{\chi}}{R^2} \right]} \pm \frac{m n_s M}{R^3} \quad (m \gg 1).$$
 (60)

For the same reasons, the second term is a small correction. If the external potential U is appropriately weak or absent, we can also omit the term U'(R):

$$|\omega_m^{\pm}| \to \frac{m^2 \sqrt{n_s \tilde{\chi}}}{R^2} \pm \frac{m n_s M}{R^3} \left(\frac{R^2 U'(R)}{\chi} \ll m^2\right), \quad (61)$$

to recover the quadratic dispersion of elementary excitations in the TQF state of a straight edge [1]. At $U'(R) \gg \chi/R^2$, there emerges a range of m values where the dispersion is linear in m and independent of χ , reflecting the fact that the potential of that strength converts the edge into a Luttinger liquid.

VI. CONCLUSION AND OUTLOOK

A two-dimensional insulating domain ("droplet") with a superclimbing edge (see Fig. 1) can be formed in a system of hard-core bosons with nearest-neighbor attraction tuned to guarantee, on the one hand, a phase-separated ground state, and, on the other hand, wide enough—and thus microscopically quantum rough—edge. The counterintuitive autonomous dynamics of such a domain is controlled by and is characteristic of the most unusual properties of TQF formed at the droplet edge.

The supertransport along the edge enables coherent (dissipation-free) displacement of the edge—the superclimbing motion. For an isolated droplet, as opposed to an infinitely long edge, or an edge with pinned ends, the superclimbing motion features fundamental modes sensitive to the presence of circulating supercurrent along the edge. In the translation invariant case and in the absence of circulating current, the droplet moves pseudo-ballistically while preserving its near circular shape—apart from slight, proportional to the square of the velocity, elongation in the transverse to the displacement direction. "Pseudo" refers to the fact that the bulk currents are zero: The insulating domain propagates in space exclusively through the matter transfer by edge supercurrents. An isotropic trapping potential converts the pseudo-ballistic motion into the sloshing mode.

The circulating supercurrent along the edge dramatically changes the droplet dynamics: The motion acquires features resembling that of a gyroscope or a two-dimensional charged particle in a perpendicular magnetic field. In a linear external potential (uniform force field), a droplet with a circulating supercurrent demonstrates a spectacular gyroscopic effect—uniform motion in the perpendicular to the force direction. This effect has a natural gyrometric aspect when the lattice

rotates; the rotation-induced phase twist results in finite supercurrent circulation in the reference frame of the lattice.

As in any superfluid, the ground state of the droplet features broken time-translation symmetry—the time-crystallization effect—manifested in the linear growth of the phase with time, $\dot{\phi}=-\mu t$. The period, $2\pi/\mu$, of the superfluid phase evolution in the ground state (dictating the frequency of the AC Josephson effect) is sensitive to the size (as well as other geometric details) of the droplet; see Eq. (42) for the case of a circle.

On the technical side, dynamics of the droplet is described by Lagrangian formalism in terms of the edge position, $\mathbf{r}(\xi,t)=(x(\xi,t),y(\xi,t))$, and the superfluid phase along the edge, $\phi(\xi,t)$, as functions of time t, with parameter ξ labeling the edge points. The structure of the Lagrangian, Eq. (22), readily follows from the continuity equation, the form of the latter expressing the law of conservation of matter under specific conditions of (i) supertransport along the edge and

(ii) insulating incompressible bulk. The two Euler-Lagrange equations implied by the Lagrangian (22) are (i) the continuity equation (14) and (ii) the generalized BJA equation (28).

Numerous other possible physical implementations of the autonomous superclimbing droplet include multicomponent bosons and higher-spin *XY*-magnets, fermionic rather than bosonic systems of ultracold atoms, ⁴He and/or ³He domains on substrates or complete layers of similar atoms, and superclimbing edge dislocation loops in ⁴He and/or ³He. Finally, similar phenomena may takes place in three dimensions with an insulating ball having a superclimbing surface.

ACKNOWLEDGMENTS

We acknowledge support from the National Science Foundation under Grants No. DMR-2335905 and No. DMR-2335904.

- [1] A. B. Kuklov, L. Pollet, N. V. Prokof'ev, and B. V. Svistunov, Supertransport by superclimbing dislocations in ⁴He: When all dimensions matter, Phys. Rev. Lett. **128**, 255301 (2022).
- [2] L. Radzihovsky, A. Kuklov, N. Prokof'ev, and B. Svistunov, Superfluid edge dislocation: Transverse quantum fluid, Phys. Rev. Lett. 131, 196001 (2023).
- [3] A. Kuklov, N. Prokof'ev, L. Radzihovsky, and B. Svistunov, Transverse quantum fluids, Phys. Rev. B **109**, L100502 (2024).
- [4] A. Kuklov, L. Pollet, N. Prokof'ev, L. Radzihovsky, and B. Svistunov, Universal correlations as fingerprints of transverse quantum fluids, Phys. Rev. A 109, L011302 (2024).
- [5] C. Zhang, M. Boninsegni, A. Kuklov, N. Prokof'ev, and B. Svistunov, Superclimbing modes in transverse quantum fluids: Signature statistical and dynamical features, arXiv:2404.03465.
- [6] M. W. Ray and R. B. Hallock, Observation of unusual mass transport in solid hcp ⁴He, Phys. Rev. Lett. 100, 235301 (2008); Observation of mass transport through solid ⁴He, Phys. Rev. B 79, 224302 (2009); Growth of solid hcp ⁴He from the superfluid, 81, 214523 (2010).
- [7] Y. Vekhov and R. B. Hallock, Mass flux characteristics in solid 4 He for $T > 100 \,\mathrm{mK}$: Evidence for bosonic Luttinger-liquid behavior, Phys. Rev. Lett. **109**, 045303 (2012).
- [8] R. B. Hallock, Mass flux experiments in solid ⁴He: Some history, recent work and the current status, J. Low Temp. Phys. 197, 167 (2019).

- [9] Z. G. Cheng, J. Beamish, A. D. Fefferman, F. Souris, S. Balibar, and V. Dauvois, Helium mass flow through a solid-superfluid-solid junction, Phys. Rev. Lett. 114, 165301 (2015).
- [10] Z. G. Cheng and J. Beamish, Compression-driven mass flow in bulk solid ⁴He, Phys. Rev. Lett. 117, 025301 (2016).
- [11] J. Shin, D. Y. Kim, A. Haziot, and M. H. W. Chan, Superfluidlike mass flow through 8 µm thick solid ⁴He samples, Phys. Rev. Lett. 118, 235301 (2017).
- [12] J. Shin and M. H. W. Chan, Mass transport through dislocation network in solid ⁴He, Phys. Rev. B 99, 140502(R) (2019).
- [13] J. Shin and M. H. W. Chan, Extinction and recovery of mass flow through solid ⁴He samples, Phys. Rev. B **101**, 014507 (2020).
- [14] M. H. W. Chan, Recent experimental studies on solid ⁴He, J. Low Temp. Phys. 205, 235 (2021).
- [15] S. G. Söyler, A. B. Kuklov, L. Pollet, N. V. Prokof'ev, and B. V. Svistunov, Underlying mechanism for the giant isochoric compressibility of solid ⁴He: Superclimb of dislocations, Phys. Rev. Lett. 103, 175301 (2009).
- [16] D. Hull and D. J. Bacon, *Introduction to Dislocations* (Butterworth-Heinemann, Elsevier, Amsterdam-Tokyo, 2011).
- [17] B. Svistunov, E. Babaev, and N. Prokof'ev, *Superfluid States of Matter* (Taylor & Francis, London, New York, 2015).